J. Eng. Technol. Sci., Vol. 53, No. 4, 2021, 210413

Characteristics of Polymeric Fiber Reinforced Cementitious Composite (PFRCC) under Uniaxial Compression

Shwan Hussain Said[1,*], Khamees Nayyef Abdulhaleem[2] & Ahmed Abdalhafedh Mustafa Al-Shaar[3]

[1,*]Technical College in Kirkuk, Northern Technical University, Mosul, Iraq
[2]Civil Engineering Department, Kirkuk University, Kirkuk, Iraq
[3]Civil Engineering Department, Al-Nahrain University, Baghdad, Iraq
[*]E-mail: shwan@ntu.edu.iq

Highlights:

- A higher reinforcing index increases the strain value and Poisson's ratio.
- The best improvement in toughness was observed for a reinforcing index of 7.9.
- The results of the mathematical model were very close to the experimental results.

Abstract: This study aimed to evaluate the compressive characteristics and toughness of polymeric fiber reinforced cementitious composites (PFRCC). In the experimental program, polyvinyl alcohol (PVA) fibers were used to prepare two groups of PFRCC cylinders with different fiber contents. The main factor considered in this study was the reinforcing index. Several parameters were investigated, i.e. compressive strength, elastic modulus, strain at peak stress, Poisson's ratio and toughness of PFRCC. The results revealed that there was a reduction in both compressive strength and elastic modulus as the reinforcing index increased, while a significant increase in the strain at peak stress was observed. Moreover, a comparison was made between different methods of toughness estimation and it was found that 7.9 was the best reinforcing index for PVA fibers based on the energy absorption performance and ductility of PFRCC. Furthermore, an empirical model is proposed in this paper to predict the PFRCC-PVA compressive stress-strain curve. The proposed model features new formulas to calculate a number of important coefficients to plot the curve based on the reinforcing index value. Besides that, the model had good convergence compared to the experimental results, with perfect values for both variance and correlation coefficient.

Keywords: *cementitious composite; compressive strength; mathematical empirical model; reinforcing index; toughness index.*

1 Introduction

A wide range of research has been conducted on the compressive behavior of steel fiber reinforced concrete. However, few studies have been done to

Received April 15th, 2020, 1st Revision November 12th, 2020, 2nd Revision January 13th, 2021, Accepted for publication April 20th, 2021.

DOI: 10.5614/j.eng.technol.sci.2021.53.4.13

investigate the compressive characteristics of the stress-strain relationship of polymeric fiber reinforced cementitious composite (PFRCC). PFRCC is a material of a group of fiber reinforced cementitious composites (FRCC), which is a particular class of concrete [1]. To improve the bendable properties and enhance the toughness and damage tolerance of FRCC, coarse aggregates are eliminated from its components [2].

Adding steel fibers to concrete enhances the strain at the peak stress and intrinsically improves its toughness [3], especially by using crimped-steel fibers with a high reinforcing index [4]. The addition of polymeric fibers has a significant role in enhancing the mechanical properties of cementitious composites. The need for polymeric fibers is growing due to their many applications, which meet the demand for sustainability [5]. The main properties of polymeric fibers are their infinitesimal diameter, high tensile strength and low specific gravity. Melt spinning is the most familiar method to produce polymeric filament fibers [6] such as poly vinyl alcohol (PVA) fibers.

The compressive stress-strain relationship of concrete allows designers and engineers to anticipate the behavior of concrete in structural applications. As a result, the performance of concrete structures is controlled by the stress-strain relationship. Eventually, addressing the parameters that affect the compressive stress-strain relationship of PFRCC is essential for designers and engineers, as information about these parameters is not extensively available. With the addition of polymeric fibers and the elimination of coarse aggregate in concrete, the cementitious composite gains a synergistic mechanical interaction between the fibers and the interfacial surface. Micromechanical material design is applicable by generating polymeric fiber reinforced cementitious composites (PFRCCs) with high ductility.

Many PFRCC applications in construction have been observed in different forms. It was found as a repair material used ably in Mitaka Dam, Japan [7], in an earth retaining wall in Gifu, Japan [8], and in an Ellsworth county road and bridge, USA [9]. The flexible material was also used to cast main parts of coupling beams in Glorio Roppongi high-rise building, Japan [10], to cast the roadbed of Mihara Bridge in Japan ([11], and to construct a bridge deck on an interstate highway in Michigan, USA [12].

In this study, different volume contents with two different aspect ratios of PVA fibers were utilized to produce PFRCC with different reinforcing indices (RI) (the reinforcing index is the result of multiplying the fiber volume content with its aspect ratio). The effect of the reinforcing index of PVA fibers on different parameters was studied, i.e. compressive strength, failure mode, modulus of elasticity, strain at peak stress, Poisson's, ratio and toughness. A comparative

study on the toughness characteristics is presented, showing different kinds of toughness evaluations. Ultimately, a mathematical empirical model is proposed to simulate the ascending and descending portion of the stress-strain curve for PFRCC in compression. Basically, the effect of different parameters, i.e. compressive strength, strain at peak stress, modulus of elasticity and reinforcing index of PVA fibers, can be evaluated with this model.

2 Experimental Program

The experimental program consisted of preparing cylindrical steel molds with a diameter of 100 mm and a height of 200 mm for producing and preparing PFRCC cylindrical specimens by incorporating polymeric PVA fibers for testing under uniaxial compressive loading. The PFRCC cylinders were cured for 28 days inside a water tank at lab temperature. The major parameters used in this program were fiber content (V_f %), and reinforcing index (V_f*l/d). Two grades of polymeric PVA fibers, RECS15-8 and RECS15-12, were used in the program, with a fiber length of 8 mm and 12 mm, respectively, and a diameter of 38 μm for both grades. As shown in Table 1, six groups of PFRCC cylinders, each includes three specimens, were produced and prepared for compressive testing using PVA RECS15 fibers according to two different aspect ratios. The first aspect ratio was equal to 200 (length of fibers = 8mm) and the second aspect ratio was equal to 316 (length of fibers = 12mm), respectively, with three

Table 1 Reinforcing indices for different groups of PFRCC.

Group symbol	Specimen symbol	Type	Aspect ratio = l/d	Fiber content V_f%	Reinforcing index
$PVAC_1$	C_{11}	RECS15-8	210	2	420
	C_{12}				
	C_{13}				
$PVAC_2$	C_{21}			2.5	525
	C_{22}				
	C_{23}				
$PVAC_3$	C_{31}			3	630
	C_{32}				
	C_{33}				
$PVAC_4$	C_{41}	RECS15-12	316	2	632
	C_{42}				
	C_{43}				
$PVAC_5$	C_{51}			2.5	790
	C_{52}				
	C_{53}				
$PVAC_6$	C_{61}			3	948
	C_{62}				
	C_{63}				

fiber contents V_f = 2, 2.5, 3% for each aspect ratio. The cement type used was type I ordinary Portland cement (SG = 3.15), fine silica sand with maximum size of particles equal to 200 micron (SG = 2.65), and fly ash type F (SG = 2.38) were used. The binder was considered as the sum weight of the cement and the fly ash. The superplasticizer (water reducer agent) used was Sika ViscoCrete 1600. The PFRCC mixing ratios and the weight of the constituents per 1 m³ are listed in Table 2.

Table 2 Mix ingredients and ratios in PFRCC specimens.

Cement C/C	Sand S/C	Fly Ash FA/C	Water W/B	(SP/B) %
1	0.8	0.28	0.355	0.31-0.34
(800)	(640)	(225)	(364)	(3.178-3.485)

Note: B = binder, i.e. cement and fly ash
( ) - by weight in kg/m^3

Figure 1 (a) and (b) show the slump test and mixing process for the PFRCC. The testing of the PFRCC cylinders was carried out at an age of 28 days using a compressive load machine a with capacity of 3000 kN, produced by Engineering Laboratory Equipment Limited (ELE), as shown in Figure 1(c). To plot the stress-train relationship for PFRCC, a compressometer with an LVDT of 5 mm travel length, was fixed at the center height of each cylinder to measure the deformation along the gauge length, as shown in Figure 1(d).

Figure 1 (a) Slump test for PFRCC mixture, (b) mixing process of PFRCC, (c) compressive load machine ELE, (d) testing setup.

Each test was continued until the load value decreased below 25% of the ultimate value. On the other hand, to obtain the static modulus of elasticity (Young's modulus) and Poisson's ratio, two rosette strain gauges, type Tee (two mutually perpendicular grids), were fixed by a special super adhesive at the middle height of the cylinders, each at the opposite side of the other. The strain gauge surface was smoothed with glass paper before fixing it. Young's modulus and Poisson's ratio were determined corresponding to 40% of the ultimate compressive strength, as illustrated in ASTM C469.

3 Results and Discussion

3.1 Compressive Stress-Strain Relationship of PFRCC

As shown in Figure 2(a), the precracking stage shows a linear elastic trend at the onset of loading until almost 40% of the compressive strength, which is a purely elastic region. Then the curve starts to deviate slightly and follow a second, so called 'elasto-plastic' region. In this region, as the compressive strength increases, the bearing deviation in the curve increases and the slope at any point gradually decreases until reaching the peak point, which represents the ultimate compressive strength. The postcracking stage also contains two regions; the first region is called the sharply descended region, which is characterized by a load, microcracks beginning to initiate within the composite structure while the the bearing load suddenly drops to an arbitrary point of about 40 to 50% of the ultimate compressive strength of the PFRCC. The drop trend is characterized by a sharp slope, which mostly decreases as the reinforcing index of the fiber increases. This region is characterized by a wide propagation of cracks in the specimen. The crack arrest mechanism of the fibers shows their role in stopping crack formation and minimizing the crack width. The second region of the postcracking stage is called the gradually descended region, which commences from the dropped point and descends in a gradual manner until an arbitrary point of failure.

Generally, the increase in the reinforcing index of the PVA fibers improves the ductility of PFRCC and thus, decreases the slope of the descended part of the curve.

3.2 Compressive Parameters of PFRCC

It is convenient to focus on the major compressive parameters and their variation with respect to the reinforcing index of PVA fibers. The static modulus of elasticity and Poisson's ratio are defined according to the requirements of ASTM C469-02. Accordingly, the static modulus of elasticity and the Poisson's ratio of PFRCC are determined based on the following equations:

$$E_c = \frac{f_c - f_i}{\epsilon_c - \epsilon_i} \quad (1)$$

$$\nu_c = \frac{\epsilon_{sc} - \epsilon_{si}}{\epsilon_c - \epsilon_i} \quad (2)$$

where E_c is the static modulus of elasticity and ν_c is Poisson's ratio; ϵ_c is the longitudinal strain value corresponding to stress value $f_c = 0.4f_c^{\backslash}$; ϵ_i is the initial longitudinal strain value = 50 x 10^{-6}; f_i is the stress value corresponding to ϵ_i; ϵ_{sc} and ϵ_{si} are the lateral strains at the mid-height of the cylinder corresponding to ϵ_c and ϵ_i.

3.3 Compressive Strength of PFRCC

The compressive strength results for the PFRCC cylinders were obtained at an age of 28 days, as illustrated in Table 3. Each magnitude recorded in this table is the mean of 3 cylinders tested in the ELE compressive test machine. Table 3 shows that the usage of PVA fibers with a higher reinforcing index in PFRCC had an undesirable influence on the compressive strength of the PFRCC. For example, an increase in the reinforcing index of PVA fibers from 4.2 to 5.25, 6.3, 7.9 and 9.48 resulted in a loss in compressive strength of about 7.14, 5.27, 6.96, 11.3 and 16.5% respectively. Figure 2(b) shows the reversed relationship of the compressive strength of the PFRCC cylinders with the reinforcing index. The regression analysis fits a linear relationship with a high correlation coefficient.

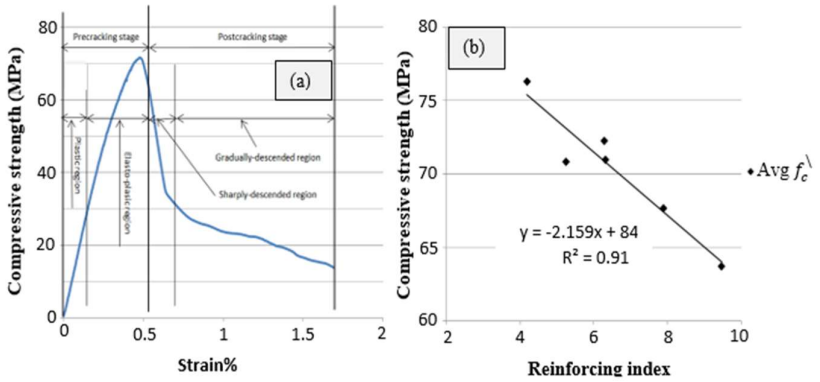

Figure 2 (a) The overall stages in a typical compressive stress-strain curve, (b) the effect of the reinforcing index of PVA fibers on the compressive strength of the PFRCC.

In the present study, the average compressive strength of the PFRCC ranged between 64 and 75.5 MPa, depending on the value of the reinforcing index, while in the study conducted by Zhao, *et al.* (2013) [13], using the same polymeric

fibers (PVA), the compressive strength was around 80 MPa. Besides, the study presented by Zhou, *et al.* (2015), using PVA fibers, showed an average compressive strength of 40 to 60 MPa, depending on the mix proportion [14]. In the study conducted by Wang, *et al.*, using hybrid fibers of steel + PVA [15], it was evaluated around 58 to 67 MPa. Mohammed, *et al.* [16] found in their study that increasing the content of PVA fibers in the mixture led to a slight decrease in compressive strength, which agrees very well with the present findings.

3.4 Failure Mode and Crack Propagation

From the literature, the cementitious mortar cylinders without fibers under compression divided, at failure, into several vertical prisms and the cracks prop ;ated vertically to the base of cylinder. In this research, Figure 3 shows the failure mode of PFRCC cylinders with respect to the reinforcing index of PVA fibers. Figure 3(a)-(f) each represent a separate sample. These samples were selected from the collection of samples tested in the experimental program, based on the reinforcing index value. The aim of these figures is to show the effect of the reinforcing index on the failure mode.

Figure 3 Failure mode and crack propagation for the cylinders in (a), (b) and (c) at lower reinforcing index, and for the cylinders in (d), (e) and (f) at higher reinforcing index of the PVA fibers.

In general, the cracks propagated diagonally, almost at 45 degrees. However, it was observed that there was an amount of splitting failure at lower values of the reinforcing index (below 6.3) associated with a small number of wide cracks due to the low bridging effect of the fibers (see Figure 3(a)-(c)). The authors Zhou, *et al.* [14] also found in their study that the failure mode of PFRCC cylinders using 2% PVA fibers propagated diagonally at 45 degrees, which agrees with the findings in the present study. The PFRCC in the mentioned study was categorized as a low reinforcing index mixture (less than 6.3) due to the low fiber content.

At higher values of the reinforcing index (6.3 and over), there was dense cracking with reduced crack width and spacing. Moreover, the splitting effect at failure was minimized or no longer observed due to the crack arrest mechanism of the fibers (see Figures 3(d)-(f)). This is ascribed to the higher bridging effect of the fibers as the reinforcing index increased. Besides that, increasing the reinforcing index gradually converts the splitting failure (which is a brittle failure) to a ductile mode of shear failure with reduced crushing effect.

3.5 Modulus of Elasticity

The modulus of elasticity determined the elastic behavior of the PFRCC specimens within the elastic range. Due to the inclusion of polymeric fibers in the PFRCC, associated with increasing the reinforcing index of PVA fibers, higher strain values were recorded within the test process. This is attributed to a better ductility of the PFRCC as the reinforcing index of the fibers increased and thus a lower value of modulus of elasticity was obtained.

PFRCC in its hardened state is a composite material designed in accordance with the concept of composite micromechanics. Accordingly, the equation stated in ACI 318M-14, Section 19.2.2 is not appropriate to calculate the modulus of elasticity because of the flexible behavior of PFRCC. Table 3 shows the reversed effect of a higher reinforcing index on the modulus of elasticity. The table reveals the fact that by increasing the reinforcing index of PVA fibers from 4.2 to 5.25, 6.3, 7.9 and 9.48, the corresponding average experimental value of the modulus of elasticity decreased by about 16.9, 22.7, 39.3, and 37.4% respectively. Figure 4(a) reveals the inverse relationship of the experimental results of the modulus of elasticity of the PFRCC PVA with the reinforcing index of fibers.

The regression analysis in the Figure fits a quadratic polynomial with high confidence. The present study showed an average elastic modulus ranging from 19 to 31 GPa, whereas the authors Zhou, *et al.* found an average value of 15 to 21 GPa [14], while a value of 19 to 21 GPa was presented by Wang, *et al.* [15]. The reduced values of the elastic modulus were due to the obtained lower

compressive strength values compared to the former values from the present study.

Table 3 Compressive parameter results for PFRCC with different reinforcing indices.

Group symbol	R. I	Specimen symbol	$f_c^{\backslash}$ Exp* MPa	$f_c^{\backslash}$ Theo+ MPa	$\varepsilon_c^{\backslash}$ Exp* *10-3	$\varepsilon_c^{\backslash}$ Theo+ *10-3	E_c Exp* GPa	E_c Theo+ GPa	ν Exp*	ν Theo+
$PVAC_1$	4.20	C_{11}	72.65	75.42	2.73	3.168	33.73	30.81	0.166	0.197
		C_{12}	76.57		3.30		28.49		0.200	
		C_{13}	79.65		3.59		30.38		0.215	
$PVAC_2$	5.25	C_{21}	68.56	73.16	3.94	3.814	21.73	26.47	0.175	0.21
		C_{22}	70.69		3.74		29.33		0.220	
		C_{23}	73.27		3.83		25.9		0.209	
$PVAC_3$	6.30	C_{31}	69.15	70.89	4.06	4.352	26.83	23.12	0.238	0.224
		C_{32}	73.04		44.0		22.52		0.219	
		C_{33}	74.62		4.57		26.04		0.204	
$PVAC_4$	6.30	C_{41}	71.47	70.89	4.82	4.352	19.91	23.12	0.249	0.224
		C_{42}	70.77		4.02		23.54		0.286	
		C_{43}	70.69		3.90		24.38		0.230	
$PVAC_5$	7.90	C_{51}	69.86	67.43	4.99	4.819	19.97	19.9	0.241	0.244
		C_{52}	65.66		4.93		16.73		0.247	
		C_{53}	67.42		4.95		19.55		0.234	
$PVAC_6$	9.48	C_{61}	66.43	64.02	4.96	4.912	18.71	18.974	0.217	0.264
		C_{62}	65.70		4.85		19.64		0.258	
		C_{63}	59.02		4.76		19.64		0.285	

Note: * = experimental value for $f_c^{\backslash}$, $\varepsilon_c^{\backslash}$, E_c and ν derived from the experimental tests

3.6 Strain at Ultimate Strength of PFRCC

The strain at ultimate strength of PFRCC is defined as the ratio between the corrected deformation of the specimen corresponding to its ultimate strength and its gauge length. As mentioned in the previous section, the strain values were increasing during the testing process until the ultimate strength of the PFRCC cylinder was reached. Accordingly, Figure 4(b) shows that the strain value at ultimate strength of PFRCC also increased along with the increase in the reinforcing index of the PVA fibers. It was observed that by increasing the reinforcing index from 4.2 to 5.25, 6.3, 7.9 and 9.48, the average strain value at ultimate strength increased by about 20, 34.2, 55 and 51.9% respectively. The best increase in average strain value was observed at a reinforcing index value of 7.9, which gave the best improvement in ductility.

The curve in Figure 4(b) fits a positive relationship of the second-degree polynomial with a high correlation coefficient. The present study revealed a peak

strain value of about 0.00317 to 0.0049, depending on the reinforcing index value, while Zhao, *et al.* (2013) [13] concluded a peak strain value of around 0.005 using PVA or polyethylene fibers. Also, the value obtained by Wang, *et al.* [15] of about 0.0045 to 0.0055 using hybrid of PVA + steel fibers, and the value obtained by Zhou, *et al.* [14] of about 0.0038 to 0.0047 using PVA fibers, were within the same range as those obtained in the present study.

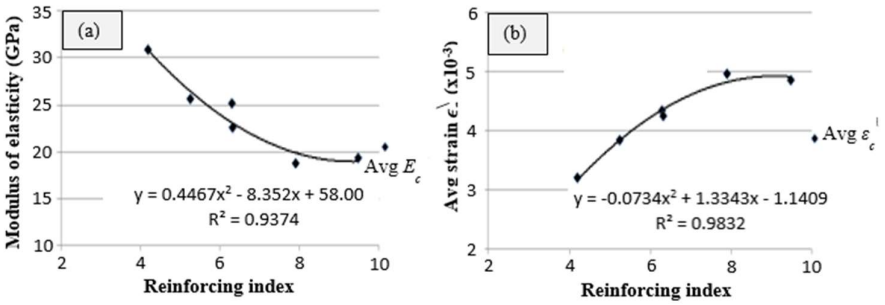

Figure 4 (a) Effect of the reinforcing index of PVA fibers on the elastic modulus of the PFRCC, (b) effect of the reinforcing index on the strain value at ultimate strength of PFRCC.

3.7 Poisson's Ratio of PFRCC

In this section, two types of Poisson's ratio are defined. The first one is the elastic Poisson's ratio. Figure 5(a) indicates that the experimental average elastic Poisson's ratio of the PFRCC mixtures is directly proportional to the reinforcing index of the PVA fibers. From Table 3 it can be seen that by increasing the reinforcing index from 4.2 to 5.25, 6.3, 7.9 and 9.48, the average elastic Poisson's ratio also increases by about 3.6, 22.4, 24.2 and 30.3%, respectively.

It is known from the literature that the value of the elastic Poisson's ratio for normal concrete varies between 0.11 and 0.21. In this study it can be seen from Table 3 that the average value for this ratio in the PFRCC mixtures varied between 0.197 and 0.264, which is 25 to 79% higher than the value in normal concrete due to the enhanced ductility of the PFRCC. On the other hand, Wang, *et al.* [15] showed a value of the Poisson's ratio of about 0.165 to 0.181 using hybrid fibers, while a value of 0.155 to 0.174 was obtained by Zhou, *et al.* [14] using PVA fibers. Poisson's ratio is a very sensitive parameter and the variation in results is due to the type and amount of fibers used and to the difference in mix proportion, which all affect Poisson's ratio.

The second type of Poisson's ratio is the cracking Poisson's ratio [17], which is observed within the elasto-plastic region of the stress-strain curve. Moreover,

Figure 5(b) shows the variation of Poisson's ratio as a function of the normalized longitudinal strain within the pre-cracking stage for some specimens with different reinforcing indeces. It can be seen from Figure 5(b) that there is a sudden increase in the cracking Poisson's ratio in the early stage of loading. Afterwards, the value of Poisson's ratio in the later stages of loading is likely to remain constant. On the other hand, Zhou, *et al*. [14] indicate that the cracking Poisson's ratio in normal concrete increases extremely within the elasto-plastic region due to the initiation of widened cracks, which propagates longitudinally and increases the strain in the lateral direction. In contrast, the PFRCC specimens were characterized by a very small crack width because the bridging mechanism of the fibers starts to activate within the elasto-plastic region and restricts the crack opening.

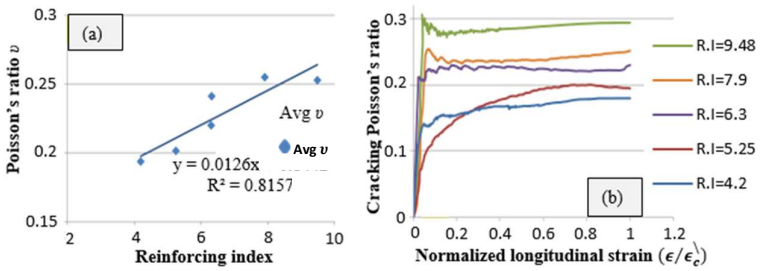

Figure 5 (a) Effect of the reinforcing index of the PVA fibers on Poisson's ratio of the PFRCC, (b) effect of the crack bridging on the value of the cracking Poisson's ratio of the PFRCC.

3.8 Compressive Toughness of PFRCC

As reported in the literature, compressive toughness is a function of the energy absorption capacity of fibrous composites under compression. The amount of absorbed energy of a specimen is simply determined by evaluation of the area under the compressive stress-strain curve. Moreover, the energy absorption capacity is a function of the ductility of the fibrous composite.

To evaluate the compressive toughness of fibrous composites, Fanella & Namaan [18] proposed a definition of the toughness index (TI), which is the ratio between the area under the compressive stress-strain curve of a fibrous composite and that of the plain matrix. In addition, Ezeldin & Balaguru [3] and Nataraja, *et al.* [4] have defined the toughness ratio (TR) as the ratio of the area under the stress-strain curve starting from the initial point of loading up to a strain of 1.5% to that of the rigid plastic material, as indicated on line DE in Figure 6(a). Furthermore, Mansour, *et al.*[19] have defined the toughness index as the ratio of the area under

the compressive stress-strain curve up to a strain of $3\epsilon_c^{\backslash}$, to the area up to a strain of $\epsilon_c^{\backslash}$, as shown on line CF in Figure 6(a).

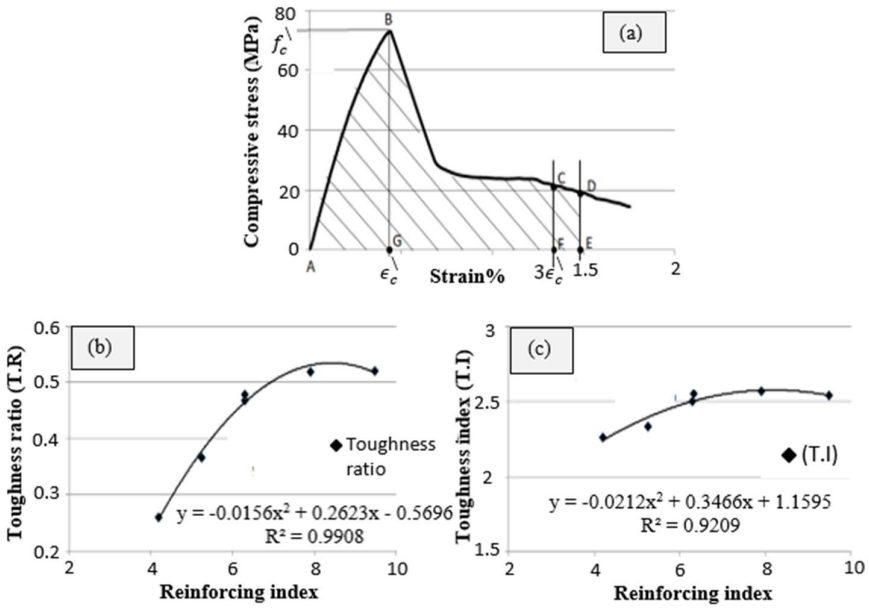

Figure 6 (a) Different definitions of the toughness index proposed by the authors, (b) effect of the reinforcing index on the toughness ratio (TR), (c) effect of the reinforcing index on the toughness index (TI).

In this study, the methods mentioned above were followed to evaluate the compressive ductility of PFRCC and to specify the best PFRCC mixture with PVA reinforcing index based on the toughness results.

The toughness ratio (TR) was calculated with the following Eq. (3) (see Figure 6(a)):

$$\text{T.R} = \frac{Area\ ABCDEFA}{0.015 * f_c^{\backslash}} \tag{3}$$

Referring again to Figure 6(a), the toughness index TI is calculated with the following Eq. (4):

$$\text{T.I} = \frac{Area\ ABCFGA}{Area\ ABGA} \tag{4}$$

Figure 6(b) indicates that by increasing the reinforcing index from 4.2 to 5.25, 6.3, 7.9 and 9.48, the average of toughness ratio of PFRCC was increased by about 41, 80, 100, and 100% respectively. It was observed that there was no improvement in the ductility at the smallest value of the reinforcing index. For the toughness index (TI) shown in Figure 6(c), as the reinforcing index increased from 4.2 to 5.25, 6.3, 7.9 and 9.48, the TI improved by about 3, 10, 13 and 12% respectively. The best improvement in toughness was observed at a reinforcing index value of 7.9, and there was no improvement in toughness at a reinforcing index value of 9.48 compared to the former value of the reinforcing index, as shown in Figure 6(c). The compressive toughness index in this study varied from 2.26 to 2.63, depending on the reinforcing index. Thus, a value of about 2.07 to 2.85 of the toughness index was concluded by Wang, *et al.* [15] using hybrid fibers, while Zhou, *et al*. [14] found a value of about 1.9 to 2.9 using PVA fibers. The wide variation observed in the toughness index value from the literature is due to the different mix proportions used by each author, while one mix proportion was used in the present study with different reinforcing indexes.

A value of 7.9 of the reinforcing index means that the optimal amount of PVA fibers incorporated in the PFRCC mix is equal to 2.5% by volume, with an aspect ratio of 316 (PVA RECS 15-12 mm) to obtain the best ductility. Finally, incorporating a higher fiber content of 3% or more, with an aspect ratio of 316 in the PFRCC mix, leads to unequal dispersion of fibers, which causes a lack of workability and homogeneity and thus a lack of ductility.

4 Proposed Mathematical Empirical Model for PFRCC

A theoretical study was presented by Cascardi, *et al.* [20] to predict the compressive stress-strain relationship of fiber reinforced polymer mortar confined columns known as an analysis-oriented model. By applying some concepts, a series of equations were solved for analyzing the data. The proposed theoretical approach found that they conformed to the experimental data with high accuracy.

In this study, it was found that the optimal formula to simulate the real behavior of PFRCC in compression is the formula presented by Carreira & Chu [21]. However, some modifications should be made to it to obtain an exact estimation with a high coefficient of correlation. The revised formula is as follows:

For the ascending part of the stress-strain curve, the normalized equation can be obtained in Eq. (5):

$$u = \frac{a_1 t}{a_1 - 1 + t^{a_2}} \tag{5}$$

where: $u = \frac{f_c}{f_c'}$, $t = \epsilon_c/\epsilon_c'$ and $a_1 = \frac{1}{1-\frac{f_c'}{\epsilon_c' E_c}}$ (6)

To determine a_1 for PFRCC, the parameters ϵ_c' and E_c should be calculated from the formulas derived from the regression analysis done on the experimental data as follows:

By referring to Table 3, Figure 4(a) and Figure 4(b), and for $59 \leq f_c' \leq 80$ MPa, $4 < \text{RI} < 10$:

$$f_c' = -2.159*(\text{RI}) + 84.49 \quad (7)$$

$$\text{Ec} = 0.4467*(\text{RI})^2 - 8.352*(\text{R.I}) + 58 \quad (8)$$

$$\epsilon_c' = (-0.0734*(\text{RI})^2 + 1.3343*(\text{RI}) - 1.1409)*10^{-3} \quad (9)$$

where RI is the reinforcing index of PVA fibers.

For each reinforcing index value, a_2 is calculated from the principle of the least squares (R^2) of the variations between the experimental data and the predicted value. By using the MATLAB software, the following equation was obtained for a_2 (referring to Figure 7):

$$a_2 = 0.0358*(\text{R.I}) + 2.2408 \quad (10)$$

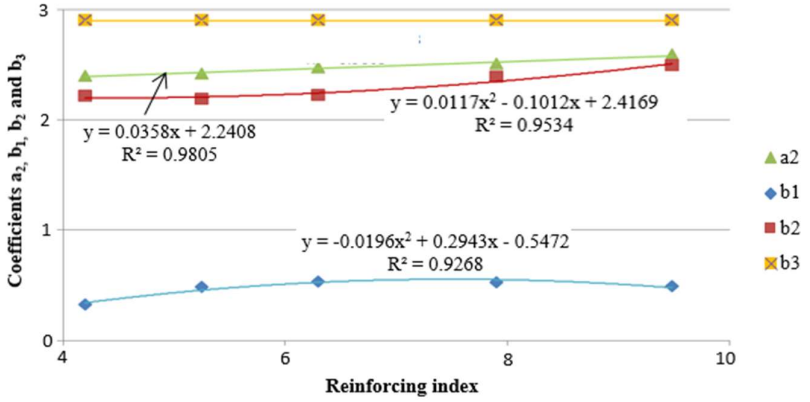

Figure 7 Variation of coefficients a2, b1, b2 and b3 with respect to the reinforcing index of the PVA fibers.

For the descending part of the stress-strain curve, the normalized equation can be obtained by Eq. (11):

$$u = \frac{b_1 t^{b_2}}{b_1 - 1 + t^{b_3}} \quad (11)$$

For each reinforcing index value, b_1, b_2 and b_3 are calculated from the principle of least squares (R^2). By applying the MATLAB software, the following equations were obtained for b_1, b_2 and b_3 (referring to Figure 7).

$$b_1 = -0.0196*(R.I)^2 + 0.2943*(R.I) - 0.5472 \quad (12)$$

$$b_2 = 0.0117*(R.I)^2 - 0.1012*(R.I) + 2.4169 \quad (13)$$

$$b_3 = 2.9 \quad (14)$$

Referring to Table 4, the highest value of variance in the proposed model for all specimens was about 0.00345, or about 0.345%, which is very low and denotes high similarity between the experimental results and the empirical model. Moreover, the coefficient of correlation R^2 ranges between 0.991 and 0.999, which is a superior value. Figures 8(a)-(f) illustrate the simulation model and the experimental results of the compressive stress-strain relationship for each group of PFRCC specimens.

Table 4 Analysis of the mathematical empirical model of compressive stress-strain.

Group symbol	R.I	Specimen	a_2 Exp*	a_2 theo+	b_1 Exp*	b_1 theo+	b_2 Exp*	b_2 theo+	Variance *10^{-3}	Correlation
PVAC1	4.2	C_{11}	2.5	2.391	0.380	0.343	2.00	2.200	2.120	0.990
		C_{12}	3.1		0.26		2.30		0.205	0.999
		C_{13}	1.70		0.334		2.35		1.625	0.995
PVAC2	5.25	C_{21}	2.35	2.429	0.580	0.458	2.00	2.208	0.521	0.999
		C_{22}	2.40		0.625		1.76		1.040	0.999
		C_{23}	2.85		0.250		2.8		2.715	0.994
PVAC3	6.3	C_{31}	2.15	2.466	0.540	0.529	2.25	2.244	0.346	0.999
		C_{32}	1.61		0.531		2.20		0.352	0.998
		C_{33}	2.08		0.600		2.00		1.261	0.998
PVAC4	6.3	C_{41}	2.81	2.466	0.525	0.529	2.2	2.244	0.3	0.999
		C_{42}	2.81		0.460		2.38		0.25	0.999
		C_{43}	3.34		0.545		2.30		0.187	0.999
PVAC5	7.90	C_{51}	2.41	2.524	0.445	0.555	2.50	2.348	0.203	0.999
		C_{52}	2.23		0.590		2.34		0.471	0.997
		C_{53}	2.9		0.537		2.33		1.846	0.995
PVAC6	9.48	C_{61}	2.60	2.580	0.440	0.481	2.53	2.510	0.276	0.998
		C_{62}	2.6		0.500		2.50		1.09	0.994
		C_{63}	2.57		0.530		2.45		1.03	0.999

Note: * = experimental values for a_2, b_1 and b_2 derived from the experimental data.
+ = theoretical values for a_2, b_1 and b_2 computed from empirical equations of the regression analysis; for all cases $b_3 = 2.9$.

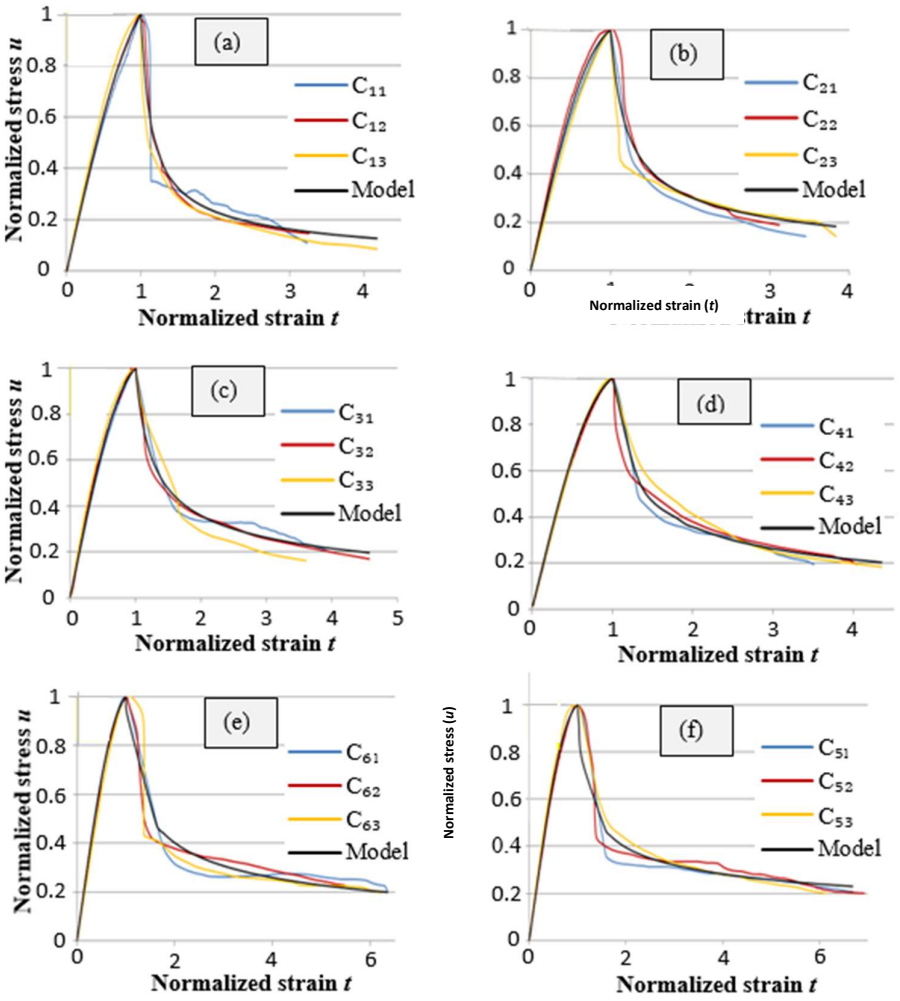

Figure 8 Compressive stress-strain relationship with modelling curve for specimens reinforced with: (a) PVA RECS15-8 mm, Vf = 2%, (b) PVA-RECS15-8 mm, Vf = 2.5%, (c) PVA-RECS15-8 mm, Vf = 3%, (d) PVA-RECS15-12 mm, Vf = 2%, (e) PVA-RECS15-12 mm, Vf = 2.5%, (f) PVA-RECS15-12 mm, Vf = 3%.

It can be concluded that the behavior of the proposed empirical model was very close to that of the experimental compressive stress-strain relationships. In addition, for all specimens that the ascending part of the model almost fully coincided with the experimental results.

5 Conclusion

Increasing the reinforcing index of PVA fibers improves the ductility of PFRCC and minimizes the slope of the descended part of the compressive stress-strain curve. Using PVA fibers with a higher reinforcing index in PFRCC results in a loss in compressive strength of about 7% to 17%, accompanied with a reduction in the average value of the modulus of elasticity of about 17% to 39%. The increment of the reinforcing index has a positive effect on the strain value at ultimate compressive strength and Poisson's ratio of about 20% to 52% and 4% to 30%, respectively.

There is a sudden increase in Poisson's ratio in the early stage of loading. For the later stages of loading, Poisson's ratio stays almost constant within the elasto-plastic range until reaching the ultimate strength of the PFRCC. The best improvement of toughness ratio TR and toughness index TI was observed at a reinforcing index of 7.9, and there was no improvement in toughness at 9.48 due to a lack of workability and homogeneity of the PFRCC and thus a lack of ductility.

A mathematical formula was proposed to simulate the behavior of PFRCC in compression with a high coefficient of correlation. Moreover, it was concluded that the behavior of the proposed mathematical empirical model was very close to the experimental compressive stress-strain results. In addition, it was observed for all specimens that the ascending part of the empirical model almost fully coincided with the experimental results. The coefficient of correlation, R, for all specimens ranged between 0.991 and 0.999, which is a superior value.

References

[1] Li, V.C. & Wang, S., *Microstructure Variability and Macroscopic Composite Properties of High Performance Fiber Reinforced Cementitious Composites*, Probabilistic Engineering Mechanics **21**, pp. 201-206, 2006.

[2] Li, V.C. & Kanda, T., *Engineered Cementitious Composites for Structural Applications*, Innovations Forum in ASCE J. Materials in Civil Engineering, **10**(2), pp. 66-69, 1998.

[3] Ezeldin, A.S. & Balaguru, P.N., *Normal- and High-strength Fiber-reinforced Concrete under Compression*, Journal of Materials in Civil Engineering, **4**(4), pp. 415-29, 1992.

[4] Nataraja, M.C., Dhang, N. & Gupta, A.P., *Stress-strain Curves for Steel-fiber Reinforced Concrete Under Compression*, Cement & Concrete Composites, **21**, pp. 383-390, 1999.

[5] Bhat, G. & Kandagor, V., *Synthetic Polymer Fibers and Their Processing Requirements*, Netherlands, Elsevier, 2014.
[6] Rawal, A. & Mukhopadhyay, S., *Melt Spinning of Synthetic Polymeric Filaments,* Netherlands, Elsevier, 2014.
[7] Li, V.C., *Engineered Cementitious Composites (ECC) – Material, Structural, and Durability Performance,* Concrete Construction Engineering Handbook, Chapter 24, E. Nawy (Ed.), CRC Press, 2008.
[8] Li, V.C., Fischer, G. & Lepech, M. D., *Shotcreting with ECC*, Spritzbeton Tagung, 2009.
[9] Li, M., *Multi-Scale Design for Durable Repair of Concrete Structures*, PhD Dissertation, University of Michigan, United States, 2009.
[10] Li, V.C., *Bendable Concrete Minimizes Cracking and Fracture Problems*, MRS Bulletin, **31**, pp. 862, 2006.
[11] Rokugo, K., Kunieda, M. and Miyazato, S., *Structural Applications of HPFRCC in Japan,* Measuring, Monitoring and Modeling Concrete Properties, an International Symposium dedicated to Professor Surendra P. Shah, Northwestern University, USA, Springer, Dordrecht, pp. 17-23, 2006.
[12] Lepech, M.D. & Li, V.C., *Application of ECC for Bridge Deck Link Slabs*, Materials and Structures, **42**, pp. 1185-1195, 2009.
[13] Zhao, Z., Sun, R., Feng, Z., Wei, S. & Huang, D., *Mechanical Properties and Applications of Engineered Cementitious Composites (ECC)*, Applied Mechanics and Materials, **405-408**, pp. 2889-2892, 2013.
[14] Zhou, J., Pan, J. & Leung, C. K. Y., *Mechanical Behavior of Fiber-reinforced Engineered Cementitious Composites in Uniaxial Compression*, Journal of Materials in Civil Engineering, **27**(1), 04014111, 2015.
[15] Wang, Z., Zuo, J., Zhang, X., Jiang, G. & Feng, L., *Stress-strain Behaviour of Hybrid-fibre Engineered Cementitious Composite in Compression*, Advances in Cement Research, **32**(2) pp. 53-65, 2020.
[16] Mohammed, B.S., Baharun, M.H., Nuruddin, M.F., Erikole, O.P.D. & Murshed, N.A., *Mechanical Properties of Engineered Cementitious Composites Mixture*, Applied Mechanics and Materials, **567**, pp. 428-433, 2014.
[17] B/525 Technical Committee Baces, *British Standard for the Design and Construction of Reinforced and Prestressed Concrete Structures, BS 8110*, Standards Board BSI, United Kingdom, 1997.
[18] Fanella, D.A. & Naaman, A.E., *Stress-Strain Properties of Fiber Reinforced Mortar in Compression*, ACI Journal, **82**(4), pp. 475-83, 1985.
[19] Mansur, M.A., Chin. M.S. & Wee, T.H., *Stress-strain Relationship of High-strength Fiber Concrete in Compression*, Journal of Materials in Civil Engineering, **11**(1), pp. 21-9, 1999.

[20] Cascari, A., Aiello, M.A. & Triantafillou, T., *Analysis-oriented Model for Concrete and Masonry Confined with Fiber Reinforced Mortar*, Materials and Structures, **50**(4), pp. 1-15, 2017.
[21] Carreira, D.J. & Chu, K.H., *Stress-strain Relationship for Plain Concrete in Compression*, Journal of the American Concrete Institute, **82**(6), pp. 797-804, 1985.